Influence of the prior athermal martensite on the mechanical response of advanced bainitic steel

Navarro-López, A.; Hidalgo Garcia, Javier; Sietsma, J.; Santofimia Navarro, Maria

DOI
10.1016/j.msea.2018.08.047

Publication date
2018

Document Version
Final published version

Published in
Materials Science and Engineering A

Citation (APA)
Navarro-López, A., Hidalgo Garcia, J., Sietsma, J., & Santofimia Navarro, M. (2018). Influence of the prior athermal martensite on the mechanical response of advanced bainitic steel. *Materials Science and Engineering A*, *735*, 343-353. https://doi.org/10.1016/j.msea.2018.08.047

Materials Science & Engineering A 735 (2018) 343–353

Contents lists available at ScienceDirect

Materials Science & Engineering A

journal homepage: www.elsevier.com/locate/msea

Influence of the prior athermal martensite on the mechanical response of advanced bainitic steel

A. Navarro-López*, J. Hidalgo, J. Sietsma, M.J. Santofimia

Department of Materials Science and Engineering, Delft University of Technology, Mekelweg 2, 2628 CD Delft, the Netherlands

ARTICLE INFO

Keywords:
Multiphase steels
Mechanical response
Isothermal treatments
Prior athermal martensite
Bainitic ferrite
Strengthening mechanisms

ABSTRACT

The accelerated formation of bainite in presence of martensite is opening a new processing window for the steel industry. However, for a feasible industrial implementation, it is necessary to determine the mechanical behaviour of the steels developed under such conditions. This study focuses on analysing the effects of the formation of athermal martensite, followed by the formation of bainitic ferrite, on the mechanical response of a low-C high-Si steel. For this purpose, microhardness measurements and tensile tests have been performed on specimens that were thermally treated either above or below the martensite-start temperature (M_s). Specimens isothermally treated below M_s exhibit a good combination of mechanical properties, comparable with that of the specimens heat treated by conventional treatments above M_s, where there was no prior formation of martensite. Investigations show an increase of the yield stress and a decrease of the ultimate tensile strength as the isothermal holding temperature is decreased below M_s. The formation of prior athermal martensite and its tempering during the isothermal holding leads to the strengthening of the specimens isothermally heat treated below M_s at the expense of slightly decreasing their strain hardening capacity.

1. Introduction

Steel industry aims to develop steels with a better balance of mechanical properties through more efficient, cost-effective, and sustainable manufacturing processes. Particularly, obtaining bainitic microstructures by the application of isothermal treatments below the martensite-start temperature (M_s) is now one of the most promising processing routes within the steel sector. This is due to the accelerating effect of the partial formation of martensite on the subsequent bainitic reaction [1–7]. These thermal treatments involve an isothermal holding below M_s after an interrupted cooling. Adequate cooling rates and alloy compositions are used to avoid the formation of ferrite, pearlite or bainite during cooling from austenitization. Bainitic ferrite forms from the untransformed austenite during the subsequent isothermal holding below M_s [6–10]. Finally, the remaining austenite will either be retained or transform into fresh martensite during the final cooling to room temperature. A multiphase microstructure is thus formed in which specific fractions of martensite and bainite coexist with carbon-enriched retained austenite.

These multiphase microstructures are comparable to the ones present in carbide-free bainitic (CFB) steels and quenching and partitioning (Q&P) steels. These steels are also developed through thermal cycles in which an isothermal holding around the M_s temperature is performed [11–15]. In CFB steels, the phase mixture is generally formed by a bainitic matrix with certain fractions of retained austenite and fresh martensite. In Q&P steels, the primary matrix is martensitic and it is tempered to some extent during the partitioning step. The final microstructure also contains certain fractions of retained austenite and fresh martensite. Regarding their mechanical behaviour, CFB and Q&P steels exhibit a composite mechanical response to the application of stress [13–15]. The relationship between their complex microstructure and their mechanical performance has been extensively studied in the last decade [11,12,14–19]. Both types of steels exhibit a good combination of strength and ductility as well as a considerable strain hardening due to the presence of high fractions of chemically stabilised retained austenite which can mechanically transform into martensite during deformation.

In multiphase steels developed through isothermal holding below M_s, the presence of prior athermal martensite leads to a different phase mixture compared to typical CFB and Q&P microstructures, which consequently affects the mechanical response of these steels. Recent studies on steels that were isothermally-treated below M_s have focused on studying the relationship between their phase mixture and their mechanical response [7,11,20–24]. Most of the reported results show an increase of the yield strength in specimens isothermally treated below M_s compared to the ones heat treated by conventional holding

* Corresponding author.
E-mail address: a.navarrolopez@tudelft.nl (A. Navarro-López).

https://doi.org/10.1016/j.msea.2018.08.047
Received 16 July 2018; Received in revised form 15 August 2018; Accepted 16 August 2018
Available online 17 August 2018

above M_s [7,11,22]. However, according to the results reported by [23], the application of isothermal holding below M_s leads to a general deterioration of the mechanical properties of the heat treated specimens. Despite the effects derived from the distinct chemical compositions of the analysed steels and the fractions of product phases formed during the isothermal holding below M_s, these diverging results can also result from the applied holding time and, consequently, from the tempering of the prior athermal martensite. In that sense, there is not a clear insight into the effects introduced by the prior athermal martensite and their significance for the mechanical response of these bainitic steels. A common observation is the refinement of the subsequently-formed bainitic ferrite [7,11,22,23]. This fact is directly related to the formation of prior athermal martensite and has been considered one of the main factors responsible for the improvement of the mechanical properties of specimens heat treated below M_s [7,22]. However, the influence of other effects resulting from the introduction of prior athermal martensite into the phase mixture, such as the precipitation of carbides due to tempering and the mechanical transformation of the unstable retained austenite, can also result decisive in the overall mechanical response of the below-M_s microstructures [20,23].

Another factor that might explain discordant results in the literature is the mechanical stability of retained austenite. The stability of austenite is affected by its composition (mainly carbon concentration), morphology, and grain size [25–27], and is generally related to the strain hardening capacity of the steel under the application of stress. The strain hardening capacity has been studied in specimens isothermally treated above and below M_s, resulting in a lower strain hardening capacity being exhibited by specimens heat treated below M_s compared to the ones treated above M_s [7,11,22,23]. This lower capacity is attributed to a lower volume fraction of blocky-shaped retained austenite (in the form of martensite-austenite (MA) islands) which potentially can transform into martensite [11,23]. Moreover, a lower strain hardening capacity is also attributed to the chemical stability of the retained austenite due to carbon enrichment. Film-shaped retained austenite is more difficult to mechanically transform into martensite than the blocky-shaped type since it can enrich from carbon more easily due to its high area to volume ratio [24]. However, this carbon enrichment of the austenite in multiphase steels isothermally treated below M_s may be also affected by the possible formation of iron carbides as a consequence of tempering of the prior athermal martensite. This phenomenon reduces the carbon concentration available to diffuse from the prior athermal martensite into the surrounding austenite, possibly leading to a less carbon enrichment of the untransformed austenite in steels isothermally treated below M_s in comparison with those treated above M_s. This latter fact has not been taken into consideration in previous research studies, so the effect of the retained austenite in the overall strain hardening capacity of multiphase steels isothermally treated below M_s remains unclear.

In this context, there is a need of performing a deeper analysis of the individual contribution of the different phases forming the multiphase matrix of these steels to their overall mechanical response. This research work mainly focuses on the effect of prior athermal martensite and its tempering during the isothermal holding on the mechanical response of multiphase steels obtained through isothermal treatments below M_s in a low-C high-Si steel, confronting with observations through conventional treatments without prior formation of martensite. Individual contributions of the different phases to the overall mechanical response are analysed in terms of grain-boundary, solid-solution, and precipitation strengthening mechanisms.

2. Experimental procedure

The chemical composition of the investigated steel is 0.2C-3.51Mn-1.52Si-0.25Mo-0.04Al (wt. pct). The as-received material was hot rolled into a 4 mm-thick steel slab. Tensile specimens were machined from the hot rolled slabs, parallel to the rolling direction. These specimens were extracted from a different area of the same hot rolled slab than that studied in previous work of the present authors [6,28]. Small local variations in the chemical composition of the extracted specimens were observed with respect the specimens used in the previous work, which gave rise to variations in the critical temperatures of the steel with respect to the values presented in [6,28].

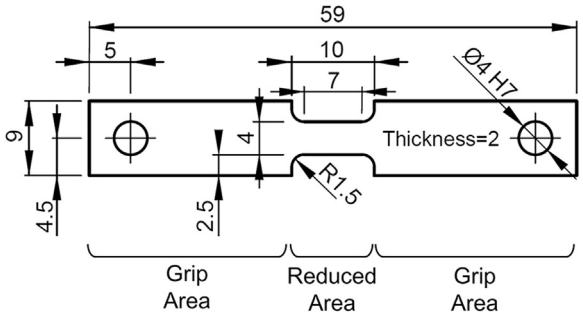

Fig. 1. Scheme of the tensile specimens (dimensions in mm).

The dimensions of the tensile specimens are shown in Fig. 1. These specimens were thermally treated with a Bähr 805 A/D dilatometer, in which heating was performed by an induction coil under a vacuum of the order of 10^{-4} mbar, and cooling by a continuous flow of helium gas. Three tensile specimens per condition were heat treated by dilatometry. Two S-type thermocouples were spot-welded to the surface of each tensile specimen: one in the middle of the reduced area (T_1) to monitor and control the temperature, and the second one in the border of the reduced area (T_2) to check the temperature gradient. The mean temperature difference measured in all specimens during austenitization and isothermal holdings was $\Delta T = T_1 - T_2 \approx 15\,^{\circ}C$.

Cylindrical dilatometry specimens were extracted from the same zone of the hot rolled slab as the tensile specimens. The dimensions of the cylinders were 10 mm in length and 3.5 mm in diameter. These specimens were heat treated with the Bähr 805 A/D dilatometer in the same conditions previously described for the tensile specimens. The heat treatments applied to tensile and cylindrical specimens are presented in Fig. 2. Dilatometry data obtained from the heat treatments performed to cylindrical specimens were used to determine the phase fractions involved in each treatment.

Vickers HV1 (1 kgf) micro-indentations were done with a DuraScan 70 (Struers) microhardness tester machine to check the homogeneity of the resulting microstructures obtained in the heat-treated tensile specimens. Average values of microhardness were obtained from three rows of equidistant indentations performed along the 7 mm gauge length of the tensile specimens. These indentations rows were separated by 1 mm, covering the total width of the gauge area.

Tensile tests were performed with an Instron 5500 R electromechanical tester machine, equipped with a maximum load cell of 100 kN, at room temperature and in extension control. The elongation during the tensile tests was recorded by a clip-on extensometer with

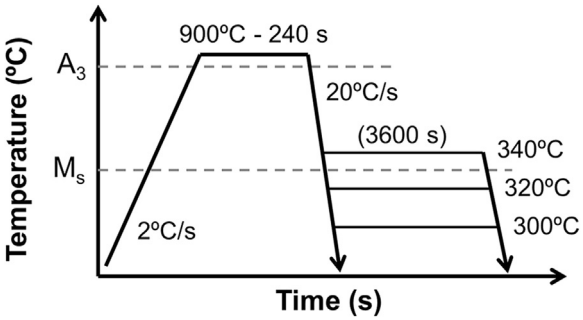

Fig. 2. Heat treatments performed by dilatometry to tensile and cylindrical specimens.

knife edges, which was attached to the tensile specimen by elastic bands. The extensometer had a gauge length of 7.8 mm with a maximum extension of ± 2.5 mm. Stress-strain curves of all specimens were obtained from the tensile tests. The yield stress (YS) was determined by the 0.2% offset method, so the yield-stress value obtained should be considered as the 0.2% proof.

Heat-treated cylindrical specimens were metallographically prepared by grinding and polishing, and etched with 2% Nital. Microstructures were analysed with a JEOL JSM-6500F Scanning Electron Microscope (SEM) using a 15 kV electron beam and the Secondary Electron Imaging (SEI) detection mode. X-ray diffraction (XRD) measurements were performed to determine the volume fraction of retained austenite (RA) and its lattice parameter at room temperature as well as the volume fraction of untransformed retained austenite after the application of uniaxial stress. The measurements were carried out using a Bruker D8-Advance diffractometer equipped with a Bruker Vantec Position Sensitive Detector. Co-Kα radiation was used in the 2θ scan from 40° to 130° with a step size of 0.035°. The fractions of austenite were calculated by the integrated area method using the (111), (200), (220), and (311) austenite peaks, and the (110), (200), (211), and (220) ferrite peaks [29]. The austenite lattice parameter was calculated by the application of the Nelson-Riley method [30] to the peak positions of the four austenite reflections.

3. Results

3.1. Phase fractions

Fig. 3.a shows the change in length as a function of temperature of the specimen directly quenched to room temperature from the austenitization conditions. The derivative of the change in length is also represented to accurately determine the M_s temperature of the studied alloy. The experimental M_s temperature at 1% volume fraction of athermal martensite was determined to be 335 °C ± 5 °C. The linear contraction during cooling from austenitization to the M_s temperature indicates the absence of formation of ferrite, pearlite, or bainite before the martensitic transformation. The dilatation occurring below the M_s temperature indicates the formation of athermal martensite. The total net dilatation caused by the athermal martensitic transformation with respect to the austenitic phase was approximately 0.88% at room temperature (indicated by a double-ended arrow in Fig. 3.a).

Fig. 3.b shows the dilatometric curves of specimens isothermally treated for one hour at 340 °C (above M_s), 320 °C, and 300 °C (below M_s). During cooling from austenitization until the isothermal holding temperature, a deviation from linearity is only observed in the dilatometry curves of specimens cooled down below M_s. This deviation indicates the formation of prior athermal martensite (PAM). The distinct martensite volume fractions formed at the two selected temperatures below M_s were calculated by applying the lever rule to the dilatometric curve of the quenched specimen. Once the isothermal temperature is reached, a dilatation takes place in all specimens during the one-hour isothermal holding applied above or below M_s, which is related to the formation of bainitic ferrite [6,28].

A non-linear change in length occurs during cooling from the isothermal temperatures to room temperature as a consequence of the formation of athermal martensite, called fresh martensite (FM) in this work, from the untransformed remaining austenite. Such martensitic transformation causes a relative net dilatation with respect to the microstructure obtained at the end of the isothermal holding, as shown by the double-ended arrow in Fig. 3.b, which allows the quantification of the fresh martensite fraction [6]. The formation of athermal martensite during the final cooling indicates the incompleteness of the isothermal bainitic transformation after one hour of holding time. A certain fraction of remaining austenite is also retained at room temperature. Volume fractions of bainitic ferrite were calculated by balancing the fractions of prior athermal martensite, fresh martensite, and retained austenite (the latter is obtained from XRD). Fig. 4 shows the volume fractions of the different phases obtained in each isothermal treatment.

3.2. Mechanical properties

The mean 0.2% offset yield stress (YS) and ultimate tensile strength (UTS) (with their standard deviations) of the tensile specimens isothermally treated at temperatures above and below M_s are presented in Fig. 4. These values were obtained from the corresponding engineering stress-strain curves (see Fig. 5). There is an opposite tendency of the YS and the UTS with the isothermal holding temperature. The specimens isothermally treated for one hour at a temperature above M_s (340 °C) exhibit lower YS and higher UTS than the ones treated at temperatures below M_s (320 °C and 300 °C), as shown in Fig. 4.

Fig. 5.a shows the engineering stress-strain curves obtained from the performed uniaxial tensile tests. Mean values of uniform elongation with their corresponding standard deviations are also shown. The directly quenched specimens exhibit the highest yield stress and ultimate tensile strength and the lowest uniform elongation and fracture strain. On the other hand, similar stress-strain engineering curves are obtained for specimens isothermally treated at temperatures above and below M_s. However, differences in yield strength can be observed in an amplified view of these engineering curves, as shown in Fig. 5.b. Moreover, for lower holding temperatures, a lower uniform elongation is

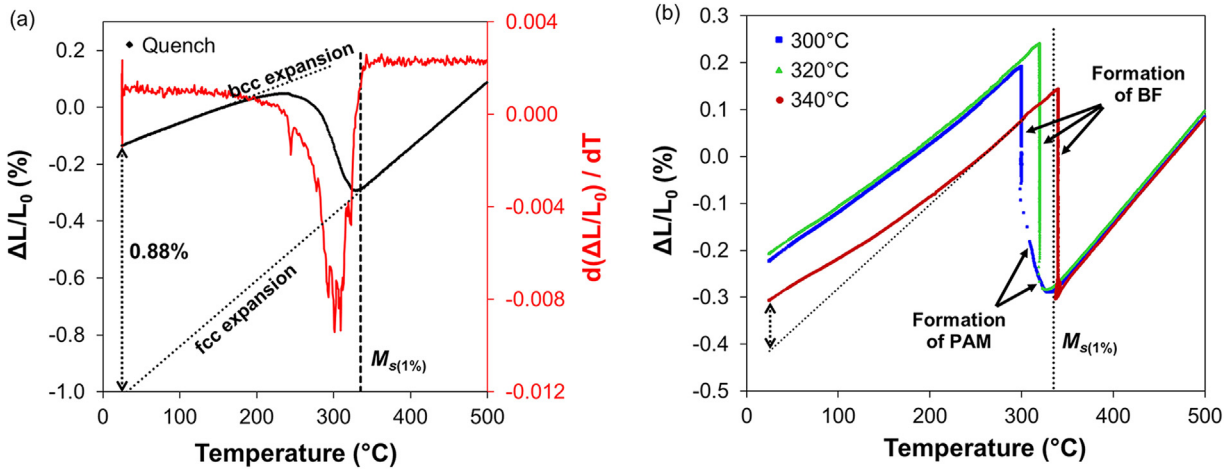

Fig. 3. Change in length as a function of temperature obtained from dilatometry measurements performed to cylindrical specimens heat treated by (a) direct quench, and (b) isothermal holding at 340 °C (above M_s), 320 °C (below M_s), and 300 °C (below M_s) for one hour.

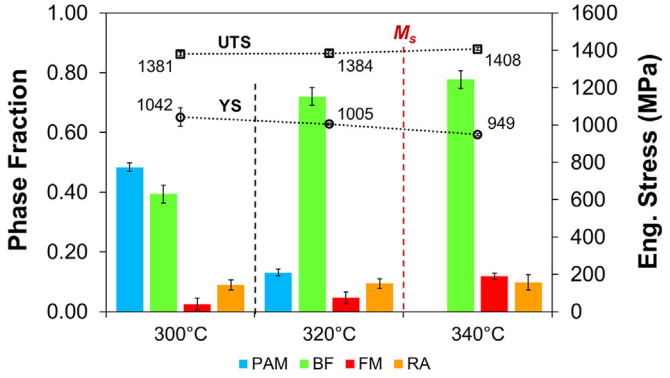

Fig. 4. Volume fractions of prior athermal martensite (PAM), bainitic ferrite (BF), fresh martensite (FM), and retained austenite (RA) obtained after the application of one-hour isothermal holdings at 340 °C (above M_s), 320 °C (below M_s), and 300 °C (below M_s). Mean values of 0.2% offset yield stress (YS) and ultimate tensile strength (UTS) exhibited by the heat-treated tensile specimens are also presented. The M_s temperature (335 °C) of the studied alloy is indicated by a dashed line.

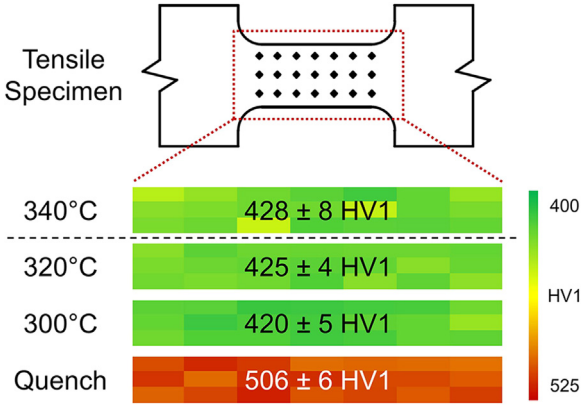

Fig. 6. Mean values of microhardness Vickers HV1 obtained from measurements performed along the gauge length of the heat-treated tensile specimens. Each group of microhardness measurements is represented by a hardness matrix, following the colours code indicated.

exhibited (see the table included in Fig. 5.a). Fracture strains are in the range of 18–23%. Note that elongation values are affected by the sub-size dimensions of the tensile specimens since a reduced gauge length leads to a significant contribution to the overall elongation from the necked region [31]. In the present work, all tensile tests were performed in sub-size specimens with exactly the same dimensions, and results were only used for the relative comparison of their mechanical response.

Fig. 5 also shows the ratio of the yield stress to the tensile strength *'YS/UTS'* for all heat-treated specimens. The *'YS/UTS'* ratio represents the capacity of a material to harden by plastic deformation and it is a widely-used parameter to determine the strain hardening potential of alloys. A lower *'YS/UTS'* ratio means that higher strain hardening will take place in the material. In this study, all heat-treated specimens exhibit *'YS/UTS'* ratios in a range of 0.67–0.75, which are typical values of strain hardening of multiphase steels [16,21]. The degree of strain hardening is lower in specimens isothermally treated below M_s.

Microhardness values Vickers HV1 of the heat-treated tensile specimens are presented in Fig. 6. In this case, microhardness values can vary from a minimum of 400 HV1 (dark green) to a maximum of 525 HV1 (dark red). Each group of measurements is represented by a hardness matrix, where each individual hardness value is assigned a specific colour within a colour scale. The hardness matrices show a uniform hardness within the gauge area for each heat-treated specimen (see Fig. 6), which is reflected in the small standard deviations obtained. These results indicate a uniform microstructure throughout the gauge of the heat-treated tensile specimens.

Quenched specimens are the hardest of the analysed heat-treated specimens. This fact is consistent with the highest UTS obtained from the engineering stress-strain curve. The microhardness of the isothermally treated specimens slightly decreases from temperatures above M_s to temperatures below M_s. This decreasing variation of the microhardness is also in agreement with the decrease of the UTS as the isothermal temperature is decreased.

3.3. Microstructures

The microstructural analysis of this work is based on a previous study of the present authors [28], which facilitates the characterization and comparison of multiphase microstructures obtained after the application of isothermal holdings above and below the M_s temperature. Fig. 7.a-d show the microstructures obtained from the quenched specimen and the one-hour isothermally treated specimens. The quenched specimen has a fully martensitic matrix which corresponds well with 97% fresh martensite fraction (calculated from XRD). Fresh martensite appears in the form of laths, with different shapes and sizes, containing carbides that grow along specific habit planes within the block-shaped substructures. The presence of carbides indicates the auto-tempering of the martensite during the fast cooling. These carbides are marked by white arrows within the magnified view of the dashed-rectangular area indicated in Fig. 7.a.

Concerning specimens isothermally treated for one hour above M_s,

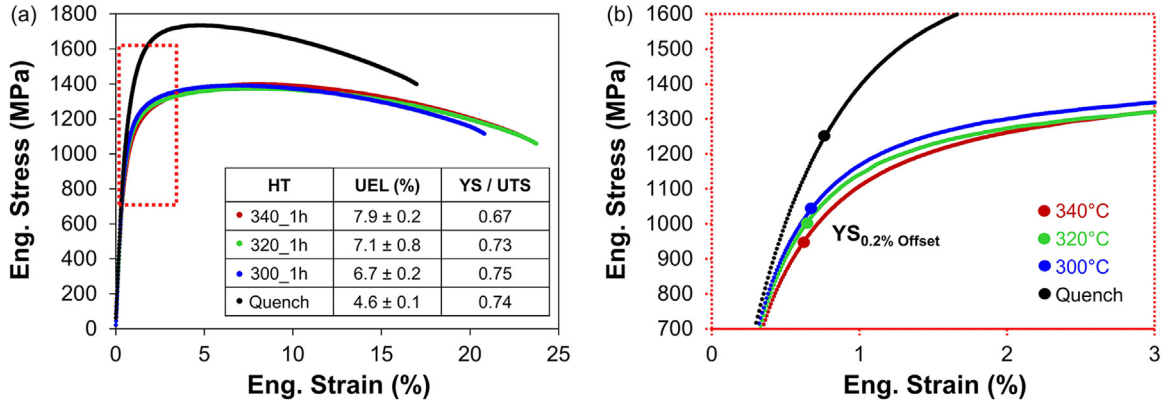

Fig. 5. (a) Engineering stress-strain curves and average values of uniform elongation (UEL) and 'YS/UTS' ratio of the tensile specimens heat-treated by a direct-quench and one-hour isothermal holdings at temperatures of 340 °C (above M_s), 320 °C, and 300 °C (below M_s); (b) Amplified view of the engineering curves (marked by a red dashed-line rectangle in (a)).

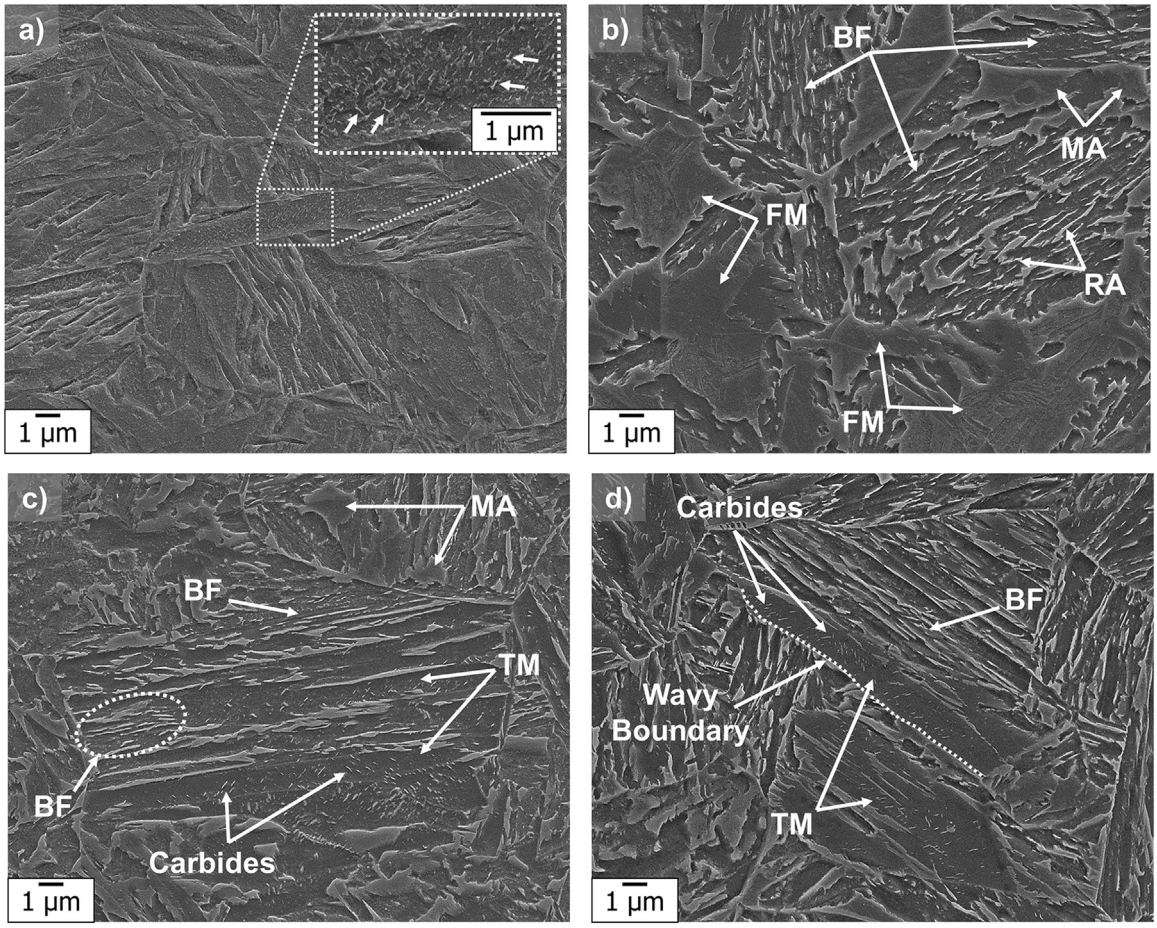

Fig. 7. Microstructures obtained after applying a) a direct-quench treatment, and isothermal treatments for one hour at the selected temperatures of b) 340 °C (above M_s), c) 320 °C (below M_s), and d) 300 °C (below M_s). BF (Bainitic Ferrite), FM (Fresh Martensite), RA (Retained Austenite), MA (Martensite-Austenite islands), and TM (Tempered Martensite, also referred as PAM).

at 340 °C, the microstructure is mainly formed by a bainitic matrix with fresh martensite areas (FM) and isolated martensite-austenite islands (MA) at the prior austenite grain boundaries (see Fig. 7.b). Bainitic ferrite (BF) appears in the form of acicular units with retained austenite films (RA) between them. Below M_s, at 320 °C, a small fraction (less than 15%) of athermal martensite was formed prior to the one-hour isothermal holding. As shown in Fig. 7.c, tempered martensite (TM) appears in the form of elongated laths with carbides within them. As occurred above M_s, acicular units of bainitic ferrite with film-like retained austenite have formed in the microstructure. Some of these acicular units appear next to the lath boundaries of tempered martensite. Fresh martensite only appears in the form of isolated martensite-austenite islands.

Finally, when the isothermal temperature is decreased to 300 °C (below M_s), a considerable volume fraction of tempered martensite (approximately 50%) is present after one hour of isothermal holding. This tempered martensite can be distinguished from bainitic ferrite, as shown in Fig. 7.d. The microstructure is then formed by a matrix of acicular units of bainitic ferrite and elongated laths of tempered martensite with wavy boundaries and carbides within them.

4. Discussion

4.1. Influence of phase mixture on strength

Specimens isothermally treated for one hour above and below M_s present similar engineering tensile curves (see Fig. 5), with maximum differences of less than 95 MPa and 30 MPa for YS and UTS, respectively. However, careful observation reveals an increase of the YS as well as a decrease of the UTS as the isothermal temperature is decreased below M_s (see Fig. 4). Since the fraction of bainitic ferrite formed at 340 °C (above M_s) and 320 °C (below M_s) is in the range of 72–78%, this evolution of the YS and UTS should be related to the formation of PAM in treatments below M_s. A qualitative analysis of the effects derived from the formation of this product phase on the overall mechanical response is presented in the following sub-sections.

4.1.1. Strengthening via refinement of structures

One of the strengthening effects is the refinement of the bainitic structures formed during isothermal holding below M_s. The formation of PAM implies three mechanisms leading to a refinement of such structures:

1) The fragmentation of the prior austenite grains formed during austenitization into smaller parts [22]. As shown in the scheme of Fig. 8, the initial austenite grain size is reduced as the volume fraction of PAM is increased, inducing the formation of finer bainitic structures.
2) The increase of the density of potential nucleation sites for bainitic ferrite introduced in the form of martensite-austenite interfaces due to the formation of PAM, which leads to an accelerating effect on its transformation kinetics [6]. The new martensite-austenite interfaces are represented as a light blue shading in Fig. 8. This refinement effect can be enhanced by the decrease of the applied isothermal temperature, which leads to a higher driving force for bainite formation [32,33].

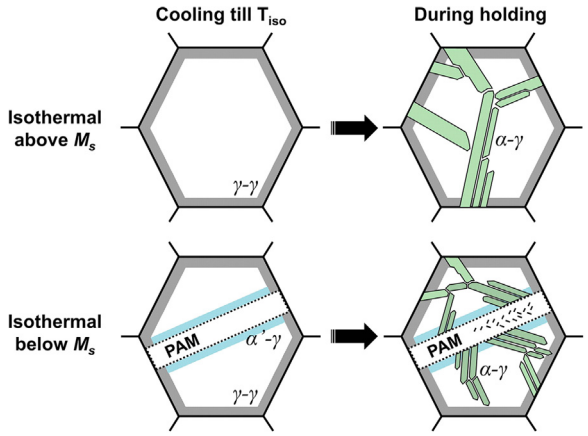

Fig. 8. Schematic representation of the refining effects caused by the formation of a certain fraction of PAM on the bainitic structures subsequently formed in isothermal holdings below M_s, in comparison with those structures formed by conventional treatments above M_s.

3) The introduction of plastic strain through the formation of PAM into the surrounding untransformed austenite. This fact leads to the strengthening of the untransformed austenite, constraining the free movement of bainite-austenite interfaces and impeding their growth [22,23].

These refinement mechanisms contribute to the grain boundary strengthening of the specimens isothermally treated for one hour below M_s. To determine the individual contribution of prior martensite laths and bainitic ferrite structures to the grain boundary strengthening of the heat treated specimens, the mean width of both types of microstructural features is estimated. The mean width of the martensitic laths (PAM), $w_{\alpha'}$, is considered as a temperature-independent value of 2.0 ± 0.6 μm (Fig. 9.a), which is extracted from previous work of the present authors [28]. This value was determined from width measurements of the same type (morphology) of martensitic laths as those described in the present work, which were characterized in specimens isothermally treated for one hour at several temperatures below M_s (270 °C, 300 °C, and 320 °C). The mean width of bainitic ferrite structures (BF), w_b, is assumed to be temperature-dependent as follows [34]:

$$w_b = w_0 \cdot \left(\frac{T - 528\ \mathrm{K}}{150\ \mathrm{K}} \right) \quad (1)$$

where T is the isothermal holding temperature in Kelvin and w_0 is a reference width. In this case, a width of 1.6 μm is considered as the reference value, which is determined from the bainitic ferrite features measured in previous work of the present authors [28]. This equation can be used for this research since the steel composition and the applied isothermal temperatures are within its validity ranges [34].

Fig. 9.a shows the estimated mean width of the bainitic ferrite structures, w_b, as a function of the applied isothermal temperature as well as the estimated width range of the prior martensite laths. The width range of bainitic ferrite structures obtained from Eq. (1) is in accordance with the width ranges of similar structures (between 0.1 and 0.8 μm) obtained through EBSD and TEM measurements by other researchers [7,11,22]. Using the values estimated by Eq. (1), the contribution of each phase to the grain boundary strengthening (σ_{gb}) of the one-hour isothermally treated specimens is obtained as

$$\sigma_{gb}^{i} \propto f^{i} \cdot (w_i)^{-1/2} \quad (2)$$

where f^i is the volume fraction of each phase obtained at the corresponding temperature and w_i is the estimated mean width of the martensitic or bainitic ferrite structures. According to general literature, a Hall-Petch type relationship as that described by Eq. (2) is applicable in micro-structured steels with grain sizes higher than 20 nm [35,36]. Eq. (2) can be thus used in the present work since the smallest size of the mean width of bainitic ferrite structures used to estimate the effect of grain refinement on the grain boundary strengthening is approximately 0.3 μm (300 nm).

Fig. 9.b shows this contribution factor as a function of the applied temperature. The contribution of bainitic ferrite structures to the strengthening of the one-hour isothermally treated specimens is higher at 320 °C than at 340 °C due to a greater refinement of a similar fraction (72–78%) of bainitic ferrite below M_s. When the isothermal temperature is decreased from 320 °C to 300 °C, the individual contribution of bainitic ferrite to the grain boundary strengthening is reduced due to the formation of a lower fraction of bainitic ferrite in comparison with that formed at 320 °C. The contribution factor of bainitic ferrite then shows a maximum at 320 °C. Fig. 9.b also displays that the strengthening contribution of the PAM increases when the temperature of the isothermal holding decreases due to an increase of the volume fraction of this product phase.

Combining these observations, and assuming the same proportionality factor in Eq. (2) for all phases, it can be concluded that, at 320 °C, the strengthening contribution of bainitic ferrite by grain refinement is higher than that of the PAM due to a great difference between the volume fractions of both product phases and to the much smaller dimensions of bainitic ferrite structures in comparison with the prior martensite laths. When decreasing the isothermal temperature to 300 °C, these differences are reduced due to the increase of the volume fraction of PAM at the expense of the bainitic ferrite volume fraction.

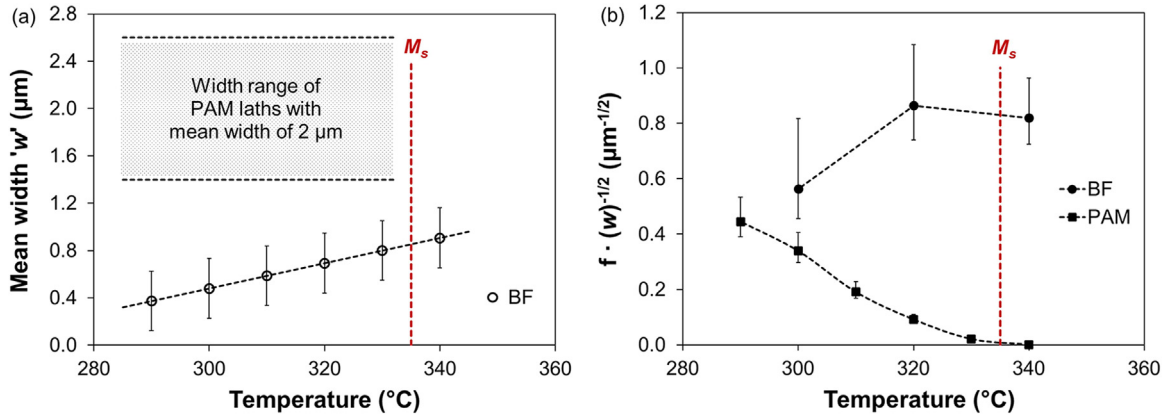

Fig. 9. (a) Mean width of prior athermal martensite (PAM) laths and bainitic ferrite structures (BF), and (b) the contribution factor from PAM and BF to the grain boundary strengthening of isothermally treated specimens as a function of the applied holding temperature.

4.1.2. Strengthening by carbon in solid solution

The yield stress can be also modified via the strengthening effect of carbon atoms and substitutional elements in solid solution within the different phases. Substitutional elements (manganese, silicon, and molybdenum) are assumed not to partition during the tempering of PAM and the isothermal formation of bainitic ferrite in all heat treatments. Therefore, the contribution of substitutional atoms to any variation of the individual strengthening of a phase is considered negligible. On the contrary, carbon in solid solution does partition between the different phases. The contribution of interstitial carbon atoms to the solid solution strengthening depends on the carbon concentration (X_C) of each individual phase. For $X_C \leq 0.2$ wt%, the contribution of the bainitic and martensitic phases can be expressed as [37]:

$$\sigma^i_{C-ss} = 1722.5 \text{ MPa/(wt\%)}^{1/2}\cdot(X^i_C)^{1/2} \quad (3)$$

while for $X_C > 0.2$ wt%, it can be calculated as [38]

$$\sigma^i_{C-ss} = 1171.3 \text{ MPa/(wt\%)}^{1/3}\cdot(X^i_C)^{1/3} \quad (4)$$

where the strength is in MPa and the concentration of carbon in solid solution of phase i is in wt%. Regarding the retained austenite, its strengthening contribution via carbon in solid solution can be determined from an empirical relation proposed by Young and Bhadeshia [39], which is expressed as [33]:

$$\sigma^{RA}_{C-ss} = 15.4 \text{ MPa/(wt\%)}\cdot(23X^{RA}_C) \quad (5)$$

where the carbon concentration in solid solution (X^{RA}_C) within the retained austenite is in wt%. To determine the contribution of each phase to the overall yield stress, the carbon concentration was first estimated as follows:

(i) Bainitic ferrite is assumed to have a carbon concentration of 0.03 wt% [39] for all isothermal treatments.

(ii) Carbon concentrations of fresh martensite were calculated from the experimental secondary M_s temperature extracted from the dilatometric curves obtained during the final cooling to room temperature (Fig. 3.b). This secondary M_s temperature depends on the carbon concentration of the remaining austenite that transforms. Carbon concentrations of secondary, fresh martensite were calculated by using the empirical equation proposed by Van Bohemen [40]

$$M_s = 565 - (31x_{Mn} + 13x_{Si} + 10x_{Cr} + 18x_{Ni} + 12x_{Mo}) - 600 \cdot[1 - \exp(-0.96x_C)] \quad (6)$$

where the secondary M_s temperature is in degrees Celsius and the concentrations of the different elements are expressed in wt%. The size reduction of the remaining austenite grains is assumed to have a negligible influence on the decrease of the secondary M_s temperature in comparison to the effect of the carbon enrichment.

(iii) The carbon concentration in the retained austenite at room temperature was calculated from [41]

$$a^\gamma = 3.572 + 0.033x_C + 0.0012x_{Mn} - 0.00157x_{Si} + 0.0056x_{Al} \quad (7)$$

where the lattice parameter a^γ is in Ångström and the concentrations of the different elements, x_i, are in wt%. The lattice parameters were determined by XRD.

(iv) The carbon concentration in solid solution within PAM was derived from additional quenching and tempering (Q&T) heat treatments. In multiphase steels, the fraction of carbon trapped in the interstitial sites of the martensite lattice can be drastically reduced during an isothermal holding. This reduction is due to the precipitation of a certain fraction of carbon atoms in the form of carbides and the diffusion of another fraction of carbon atoms from the PAM into the surrounding untransformed austenite. The aim of these additional Q&T treatments is to create a fully martensitic matrix tempered in similar temperature-time conditions as the PAM obtained in the isothermally treated specimens below M_s. Since no significant carbon partitioning to austenite takes place in the Q&T microstructure, the determination of the final carbon concentration in tempered martensite for each temperature-time condition will be considered as the maximum carbon concentration that PAM can contain in solid-solution after the one-hour isothermal treatments at the same temperatures.

Quenching and tempering (Q&T) treatments were carried out in the dilatometer by a direct quench from austenitization to room temperature, followed by a tempering stage of one hour at 320 °C and/or 300 °C. The microstructure obtained in both Q&T treatments was formed by a 0.97–0.98 volume fraction of tempered martensite and a 0.02–0.03 fraction of retained austenite. X-ray diffraction measurements were performed to determine the BCC lattice parameter, which, in this case, corresponds to the lattice parameter of the one-hour tempered martensite since no other BCC-phases formed in Q&T treatments. The carbon concentration in tempered martensite was calculated using [42]

$$X^{TM}_C = 31 \text{ wt.\%/Å}\cdot(a^{TM} - a^\alpha) \quad (8)$$

where a^{TM} is the lattice parameter of the tempered martensite and a^α is the lattice parameter of a reference sample, containing no carbon in the BCC phase, with a value of 2.866 Å [43].

Applying Eq. (8), the carbon concentration in solid solution of the tempered martensite formed in Q&T treatments at temperatures of 320 °C and 300 °C (below M_s) was 0.08 and 0.09 wt%, respectively. This loss of carbon in solid solution within the initial carbon-supersaturated martensite is mainly attributed to the formation of carbides during tempering. The volume fraction of retained austenite is so small that the fraction of carbon atoms diffusing from tempered martensite to retained austenite is considered negligible in Q&T treatments.

Table 1 shows the balance of phase fractions and their corresponding carbon concentrations ($X_{C\text{-}ss}$) of the specimens isothermally treated at temperatures above and below M_s. A certain concentration of carbon atoms ($X_{C\text{-}prec.}$) is considered to precipitate as carbides during the isothermal holding since micrographs of specimens isothermally treated below M_s (see Fig. 7.c-d) show their presence within the tempered laths of PAM. Note that a certain fraction of carbides can also be present within phases such as bainitic ferrite and fresh martensite obtained in treatments above and below M_s. The final balance of carbon concentrations was obtained by applying the equation:

$$X_{CT} = 0.2 = \sum (f^i\cdot X^i_{C-ss}) + (X_{C-prec.}) \quad (9)$$

where f^i represents the volume fraction of the phase i (prior athermal martensite, bainitic ferrite, fresh martensite, or retained austenite), and the quantities X_{CT}, $X_{C\text{-}ss}$, and $X_{C\text{-}prec.}$ are the nominal carbon concentration of the steel (in this case, 0.2 wt%), the carbon concentration in solid solution of the phase i, and the carbon concentration in the form of carbides, respectively.

The individual strengthening contributions by carbon atoms in solid solution (σ_{ss}) of the prior athermal martensite, bainitic ferrite, fresh martensite, and retained austenite were calculated by

$$\sigma^i_{ss} = f^i\cdot\sigma^i_{C-ss} \quad (10)$$

where f^i is the experimental volume fraction of each phase and $\sigma_{C\text{-}ss}$ is the contribution of the solute carbon atoms calculated from Eqs. (3)–(5).

Fig. 10.a shows the corresponding individual contributions of PAM, bainitic ferrite (BF), fresh martensite (FM), and retained austenite (RA) to the strengthening by solute carbon atoms in the isothermally treated specimens at temperatures above and below M_s. All heat treated specimens present a small and similar strengthening by carbon in solid solution derived from the presence of retained austenite. Despite retained austenite exhibiting the highest carbon concentration between all phases (see Table 1), its strengthening contribution by solute carbon

Table 1
Phase fractions (f^i) and carbon concentrations in wt% (X_C) of the prior athermal martensite (PAM), bainitic ferrite (BF), fresh martensite (FM), and retained austenite (RA) of specimens isothermally treated at 340 °C (above M_s), 320 °C (below M_s), and 300 °C (below M_s). The sum of the products of the phase fractions (PAM, BF, FM, and RA) by their respective es. The remaining carbon concentration is considered to be in the form of carbides.

HT	PAM		BF		FM		RA		$\Sigma(f^i X_{C\text{-}ss})$ (wt%)	$X_{C\text{-}prec.}$ (wt%)	X_{CT} (wt%)
	f^{PAM}	$X_{C\text{-}ss}$	f^{BF}	$X_{C\text{-}ss}$	f^{FM}	$X_{C\text{-}ss}$	f^{RA}	$X_{C\text{-}ss}$			
340 °C	0.00 ± 0.00	0.00	0.78 ± 0.03	0.03	0.12 ± 0.01	0.41	0.10 ± 0.03	0.91	**0.16**	**0.04**	**0.20**
320 °C	0.13 ± 0.01	0.08	0.72 ± 0.03	0.03	0.05 ± 0.02	0.59	0.09 ± 0.02	0.91	**0.15**	**0.05**	**0.20**
300 °C	0.48 ± 0.01	0.09	0.39 ± 0.03	0.03	0.03 ± 0.02	0.65	0.09 ± 0.02	0.85	**0.15**	**0.05**	**0.20**

atoms results to be not significant compared to the individual contributions of the other phases at the three selected temperatures. At 340 °C (above M_s), the main strengthening contribution stems from the bainitic ferrite due to its high volume fraction. The second greatest contribution derives from the 12% volume fraction of fresh martensite and represents approximately 30% of the total strengthening contribution.

At 320 °C (below M_s), the main contribution to solid-solution strengthening also comes from the bainitic ferrite since it represents 72% of the total phase fraction. This contribution is similar to that of the bainitic ferrite at 340 °C due to similar volume fractions (in the range of 72–78%). At this lower temperature, the presence of a certain fraction of PAM also contributes to the overall solid-solution strengthening of the heat-treated specimens, compensating to some extent the lower contribution exhibited by 5% of fresh martensite. The sum of individual contributions of the different phases to the overall strengthening of the specimens isothermally treated at 320 °C is not significantly different to that obtained at 340 °C (see Fig. 10.a).

At 300 °C (below M_s), as a higher fraction of PAM is formed, the individual contribution by carbon in solid solution of this product phase becomes dominant within the multiphase matrix. As observed in Fig. 10.a, a similar strengthening contribution by carbon in solid solution is obtained with 48% volume fraction of PAM formed in specimens isothermally treated at 300 °C than with 78% volume fraction of bainitic ferrite formed in those treated at 340 °C. This means that formation of PAM has a greater effect than bainitic ferrite on the overall solid-solution strengthening of the isothermally treated specimens below M_s.

Fig. 10.b shows a comparison of the individual strengthening contributions by carbon in solid-solution of the prior athermal martensite, bainitic ferrite, and fresh martensite as a function of their volume fraction. The solid-solution strengthening contribution of PAM to the overall yield stress per unit of fraction is 1.7 times higher than that of the bainitic ferrite. This relationship is directly dependent on the carbon concentrations attributed to PAM and bainitic ferrite. If the diffusion of carbon from the PAM to the remaining untransformed austenite is also considered to occur during the isothermal holding, the strengthening contribution of PAM will decrease as a consequence of the additional reduction of its carbon concentration in solid solution; this decrease is represented by blue arrows in Fig. 10.b. Then, differences (shaded area) between the individual strengthening contributions via carbon in solid solution of PAM and bainitic ferrite will be smaller.

Maintaining a similar fraction of bainitic ferrite (72–78%), there is a decrease of the UTS as the isothermal temperature is decreased from 340 °C to 320 °C (see Fig. 4). This is mainly due to the reduction of the fresh martensite fraction formed (which is the hardest phase) as well as the formation of a certain fraction of PAM at 320 °C (which is tempered). When the isothermal temperature is decreased from 320 °C to 300 °C, the UTS remains almost constant (see Fig. 4) in spite of the variations of the fractions of PAM and bainitic ferrite. During the isothermal holding below M_s, the PAM reduces its carbon concentration by carbide precipitation and presumably also reduces its dislocation density, leading to a softening of this product phase. In both specimens, the sum of volume fractions of PAM and bainitic ferrite is approximately 85–87%, confirming that tempered PAM may have a similar influence on the UTS as the isothermally formed bainitic ferrite.

The formation of carbides by the precipitation of part of the carbon contained within the PAM acts as a strengthening mechanism of the specimens heat treated below M_s, partly compensating the strengthening decrease by the loss of carbon in solid solution. This precipitation strengthening, together with the grain boundary strengthening, leads to an increase of the yield stress of these specimens with respect the ones

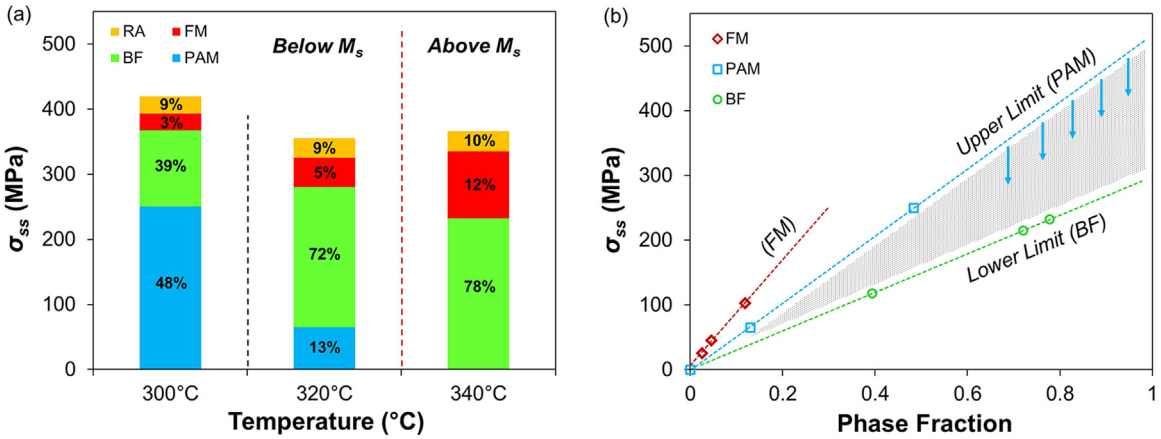

Fig. 10. Comparison of the product of the volume fractions and the individual strengthening contributions by carbon in solid solution of the prior athermal martensite (PAM), bainitic ferrite (BF), and fresh martensite (FM) as a function of (a) the isothermal temperature and (b) the phase fraction. The numbers in percentage indicated in (a) correspond to the volume fractions of each phase.

heat treated above M_s. In turn, precipitation strengthening can imply the softening of the phase(s) in which carbides are contained, explaining the decrease of the UTS of the specimens heat treated below M_s.

4.2. Influence of phase mixture on strain hardening

Fig. 5 shows an increase of the YS/UTS ratio as the isothermal temperature is decreased from above M_s to below M_s, which implies a decrease of the strain hardening potential in specimens isothermally treated below M_s. This decreasing tendency is consistent with the observations of other researchers in similar studies [7,11,22,23]. In order to understand this tendency, two microstructural aspects are considered: (i) the presence of tempered PAM in these heat treated specimens and (ii) the possible differences in the mechanical stability of the retained austenite compared to the specimen heat treated above M_s. These aspects are discussed below:

(i) The presence of tempered PAM in the phase mixture of specimens heat treated below M_s gives rise to two opposing effects. On the one hand, PAM has a softer character than the fresh martensite obtained during the final cooling to room temperature due to the reduction of its carbon concentration in solid solution and a presumable reduction in dislocation density. Both phenomena are a direct consequence of the tempering process and lead to a decrease in UTS. On the other hand, the presence of higher fractions of tempered PAM with the decreasing annealing temperature lead to an increase of the yield stress due to a greater presence of carbides, compared to bainitic microstructures. These carbides can act as pinning points of the dislocations, impeding their movement. The combination of both effects narrows the difference between YS and UTS to the decreased capacity of plastic deformation of specimens isothermally treated below M_s.

(ii) The volume fractions of retained austenite (obtained by XRD) present in the isothermally treated specimens before and after performing the uniaxial tensile tests are shown in Fig. 11. Results indicate that about 2/3 of the total volume fraction of retained austenite is mechanically transformed during the application of stress in all heat treated specimens. These observations suggest that the mechanical transformation of the retained austenite in multiphase microstructures is contributing in a similar way to the strain hardening of all heat treated specimens. However, slight differences in the mechanical stability of the retained austenite are due to variations in its composition, size, and morphology, but also to the strength of the surrounding phase [44–47].

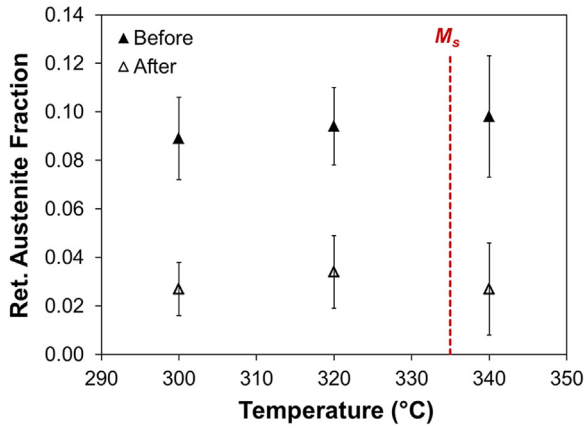

Fig. 11. Volume fraction of retained austenite contained in specimens isothermally treated at the three selected temperatures above and below M_s before and after the application of tensile tests.

High and similar carbon concentrations in the retained austenite are exhibited by all heat treated specimens (see Table 1) as a consequence of the carbon enrichment of the untransformed austenite during the isothermally bainite formation. These carbon concentrations should be sufficiently high to hinder the mechanical transformation of the retained austenite up to reaching the yield stress [48–51], so austenite transformation is assumed to effectively contribute to the strain hardening capacity. Small differences in the strain hardening contribution of the retained austenite between specimens heat treated at the three selected temperatures may be related to the mechanical stability of the distinct types of retained austenite present in these multiphase microstructures (see Fig. 7.b-d). Thin films of retained austenite are mechanically more stable than coarser blocky grains of austenite in bainitic steels obtained through conventional treatments above M_s [52]; moreover, coarser grains are easier to mechanically transform than smaller ones. However, further investigations are needed to elucidate the individual contribution of the different types of retained austenite to the strain hardening of the heat treated specimens.

The analysis of the mechanical stability of retained austenite within these multiphase microstructures shows that the individual contribution of the mechanically-induced transformation of the retained austenite to the strain hardening capacity is similar in specimens heat treated above and below M_s due to the formation of similar fractions of retained austenite with similar levels of carbon enrichment and the transformation of similar fractions of retained austenite into martensite under the application of stress. At the same time, the formation and tempering of PAM gives rise to a lower strain hardening capacity of specimens annealed at temperatures below M_s. Combining both observations, it is concluded that the presence of tempered PAM within the multiphase microstructure slightly reduces the strain hardening capacity of specimens heat treated below M_s compared to those treated above M_s since tempered PAM counteracts the contribution of the mechanical transformation of the retained austenite.

5. Conclusions

The effects derived from the formation and tempering of prior athermal martensite on the overall mechanical response of a low-C high-Si steel were studied in terms of grain-boundary, solid-solution, and precipitation strengthening mechanisms in specimens isothermally treated for one hour at temperatures below M_s and confronted, in similar terms, with observations extracted from conventional treatments performed above M_s, where athermal martensite is not formed prior to the isothermal holding. The main conclusions obtained are the following:

1. Specimens isothermally treated for one hour below M_s exhibit higher yield stress and lower ultimate tensile strength than those treated by conventional heat treatments above M_s. Since the gap between yield stress and ultimate tensile strength is narrowed with the decreasing annealing temperature, specimens that were isothermally treated below M_s exhibit a smaller capacity of strain hardening during deformation than the ones treated above M_s.
2. The formation of small fractions of prior athermal martensite leads to an increase of the yield stress of the specimens treated below M_s with similar volume fractions of bainitic ferrite as those treated above M_s. This increasing tendency continues with the decreasing annealing temperature due to the formation of higher fractions of prior athermal martensite at the cost of bainitic ferrite and fresh martensite.
3. The formation of prior athermal martensite and its tempering during the one-hour isothermal holdings below M_s triggers several strengthening mechanisms, favouring the increase of the yield stress of these multiphase specimens. These phenomena are: the introduction of martensite-austenite interfaces, the presence of a higher carbon concentration in solid solution in prior athermal

martensite (compared to bainitic ferrite), and the formation of carbides within laths of prior athermal martensite during the isothermal holding.

4. There is a similar contribution of the mechanical transformation of the retained austenite, upon the application of uniaxial stress, to the strain hardening of multiphase microstructures obtained by one-hour isothermal holdings above and below M_s. However, the presence and tempering of prior athermal martensite counteract this contribution in specimens heat treated below M_s and, consequently, slightly reduce their strain hardening capacity. This mainly occurs due to the softening of the tempered PAM as consequence of losing carbon in solid-solution (decreasing ultimate tensile strength) and the higher presence of carbides as the volume fraction of PAM is increased within the phase mixture (increasing yield stress).

Acknowledgements

The authors would like to thank Dr. Carola Alonso de Celada for her advice and fruitful discussions, and Richard Huizenga for the X-ray diffraction analysis. The authors gratefully acknowledge the financial support of the Netherlands Organization for Scientific Research (NWO) and the Dutch Foundation for Applied Sciences (STW) through the VIDI-Grant 12376.

Data availability

The raw and processed data required to reproduce the findings of this research study are available to download from the Supplementary material.

Appendix A. Supporting information

Supplementary data associated with this article can be found in the online version at doi:10.1016/j.msea.2018.08.047.

References

[1] R.T. Howard, M. Cohen, Austenite transformation above and within the martensite range, Trans. AIME 176 (1948) 384–397.
[2] C.E. Ericsson, M.S. Bhat, E.R. Parker, V.F. Zackay, Isothermal studies of bainitic and martensitic transformations in some low alloy steels, Metall. Trans. A 7 (1976) 1800–1803.
[3] D.H. Kim, J.G. Speer, H.S. Kim, B.C. de Cooman, Observation of an isothermal transformation during quenching and partitioning processing, Metall. Mater. Trans. A 40 (2009) 2048–2060.
[4] H. Kawata, K. Hayashi, N. Sugiura, N. Yoshinaga, M. Takahashi, Effect of martensite in initial structure on bainite transformation, Mater. Sci. Forum 638–642 (2010) 3307–3312.
[5] M.J. Santofimia, S.M.C. van Bohemen, D.N. Hanlon, L. Zhao, J. Sietsma. Perspectives in high-strength steels: Interactions between non-equilibrium phases, in: Proceedings of the Inter. Symp. on AHSS, 2013, AIST, pp. 331–339.
[6] A. Navarro-López, J. Sietsma, M.J. Santofimia, Effect of prior athermal martensite on the isothermal transformation kinetics below M_s in a Low-C High-Si Steel, Metall. Mater. Trans. A 47 (2016) 1028–1039.
[7] L. Zhao, L. Qian, J. Meng, Q. Zhou, F. Zhang, Below-M_s austempering to obtain refined bainitic structure and enhanced mechanical properties in low-C high-Si/Al steels, Scr. Mater. 112 (2016) 96–100.
[8] P. Kolmskog, A. Borgenstam, M. Hillert, P. Hedstrom, S.S. Babu, H. Terasaki, Y.I. Komizo, Direct observation that bainite can grow below M_s, Metall. Mater. Trans. A 43A (2012) 4984–4988.
[9] E.P. Da Silva, D. De Knijf, W. Xu, C. Föjer, Y. Houbaert, J. Sietsma, R. Petrov, Isothermal transformations in advanced high strength steels below martensite start temperature, Mater. Sci. Technol. 31 (2015) 808–816.
[10] S. Samanta, P. Biswas, S. Giri, S.B. Singh, S. Kundu, Formation of bainite below the M_s temperature: kinetics and crystallography, Acta Mater. 105 (2016) 390–403.
[11] J.C. Hell, M. Dehmas, S. Allain, J.M. Prado, A. Hazotte, J.P. Chateau, Microstructure-properties in carbide-free bainitic steels, ISIJ Int. 51 (2011) 1724–1732.
[12] X.Y. Long, J. Kang, B. Lu, F.C. Zhang, Carbide-free bainite in medium carbon steel, Mater. Des. 64 (2014) 237–245.
[13] J. Sun, H. Yu, S. Wang, Y. Fan, Study of microstructural evolution, microstructure-mechanical properties correlation and collaborative deformation-transformation behaviour of quenching and partitioning (Q&P) steel, Mater. Sci. Eng. A 596 (2014) 89–97.
[14] I. de Diego-Calderón, D. De Knijf, M.A. Monclus, J.M. Molina-Aldareguia, I. Sabirov, C. Föjer, R.H. Petrov, Global and local deformation behaviour and mechanical properties of individual phases in a quenched and partitioned steel, Mater. Sci. Eng. A 630 (2015) 27–35.
[15] F. HajyAkbary, J. Sietsma, G. Miyamoto, N. Kamikawa, R. Petrov, T. Furuhara, M.J. Santofimia, Analysis of the mechanical behaviour of a 0.3C-1.6Si-3.5Mn quenching and partitioning steel, Mater. Sci. Eng. A 677 (2016) 505–514.
[16] E.P. Bagliani, M.J. Santofimia, L. Zhao, J. Sietsma, E. Anelli, Microstructure, tensile and toughness properties after quenching and partitioning treatments of a medium-carbon steel, Mater. Sci. Eng. A 559 (2013) 486–495.
[17] I. de Diego-Calderón, M.J. Santofimia, J.M. Molina-Aldareguia, M.A. Monclus, I. Sabirov, Deformation behaviour of a high strength multiphase steel at macro- and micro- scales, Mater. Sci. Eng. A 611 (2014) 201–211.
[18] D. De Knijf, R. Petrov, C. Föjer, L.A.I. Kestens, Effect of fresh martensite on the stability of retained austenite in quenching and partitioning steel, Mater. Sci. Eng. A 615 (2014) 107–115.
[19] K.O. Findley, J. Hidalgo, R.M. Huizenga, M.J. Santofimia, Controlling the work hardening of martensite to increase the strength/ductility balance in Q&P steels, Mater. Des. 117 (2017) 248–256.
[20] X. Tan, Y. Xu, X. Yang, D. Wu, Microstructure-properties relationship in a one-step quenched and partitioned steel, Mater. Sci. Eng. A 589 (2014) 101–111.
[21] G. Mandal, S.K. Ghosh, S. Bera, S. Mukherjee, Effect of partial and full austenitisation on microstructure and mechanical properties of quenching and partitioning steel, Mater. Sci. Eng. A 676 (2016) 56–64.
[22] J. Feng, T. Frankenbach, M. Wettlaufer, Strengthening 42CrMo4 steel by isothermal transformation below martensite start temperature, Mater. Sci. Eng. A 683 (2017) 110–115.
[23] J. Tian, G. Xu, M. Zhou, H. Hu, Refined bainite microstructure and mechanical properties of a high-strength low-carbon bainitic steel treated by austempering below and above M_s, Steel Res. Int. (2018) 1–10.
[24] A. Zinsaz-Borujerdi, A. Zarei-Hanzaki, H.R. Abedi, M. Karam-Abian, H. Ding, D. Han, N. Kheradmand, Room temperature mechanical properties and microstructure of a low alloyed TRIP-assisted steel subjected to one-step and two-step quenching and partitioning process, Mater. Sci. Eng. A 725 (2018) 341–349.
[25] Z.C. Li, H. Ding, R.D.K. Misra, Z.H. Cai, Microstructure-mechanical property relationship and austenite stability in medium-Mn TRIP steels: the effect of austenite-reverted transformation and quenching-tempering treatments, Mater. Sci. Eng. A 682 (2017) 211–219.
[26] D. De Knijf, C. Föjer, L.A.I. Kestens, R. Petrov, Factors influencing the austenite stability during tensile testing of quenching and partitioning steel determined via in-situ Electron Backscatter Diffraction, Mater. Sci. Eng. A 638 (2015) 219–227.
[27] R.D.K. Misra, V.S.A. Challa, P.K.C. Venkatsurya, Y.F. Shen, M.C. Somani, L.P. Karjalainen, Interplay between grain structure, deformation mechanisms and austenite stability in phase-reversion-induced nanograined/ultrafine-grained austenitic ferrous alloy, Acta Mater. 84 (2015) 339–348.
[28] A. Navarro-López, J. Hidalgo, J. Sietsma, M.J. Santofimia, Characterization of bainitic-martensitic structures formed in isothermal treatments below the M_s temperature, Mater. Charact. 128 (2017) 248–256.
[29] C.F. Jatczak, J.A. Larson, S.W. Shin, Retained austenite and its measurements by X-ray diffraction, Soc. Automot. Eng. (1980) 453 (Special Publication).
[30] J.B. Nelson, D.P. Riley, An experimental investigation of extrapolation methods in the derivation of accurate unit-cell dimensions of crystals, Proc. Phys. Soc. 56 (1945) 160–176.
[31] G.E. Dieter, Mechanical Metallurgy, SI Metric Edition, McGraw-Hill, 1988.
[32] L.C. Chang, H.K.D.H. Bhadeshia, Austenite films in bainitic microstructures, Mater. Sci. Technol. 11 (1995) 874–881.
[33] S.B. Singh, H.K.D.H. Bhadeshia, Estimation of bainite plate-thickness in low-alloy steels, Mater. Sci. Eng. A 245 (1998) 72–79.
[34] H. Matsuda, H.K.D.H. Bhadeshia, Kinetics of the bainite transformation, Proc. R. Soc. Lond. A 460 (2004) 1707–1722.
[35] H.K.D.H. Bhadeshia, R.W.K. Honeycombe, Steels: Microstructure and Properties, 4th ed., Elsevier Ltd, 2017, pp. 41–42.
[36] S.H. Whang, Nanostructured Metals and Alloys: Processing, Microstructure, Mechanical Properties and Applications, 1st ed., Woodhead Publishing Limited, 2011.
[37] G.R. Speich, H. Warlimont, Yield strength and transformation substructure of low-carbon martensite, J. Iron Steel Inst. 206 (1968) 385–392.
[38] P.G. Winchell, M. Cohen, The strength of martensite, Trans. ASM 55 (1962) 347–361.
[39] C.H. Young, H.K.D.H. Bhadeshia, Strength of mixtures of bainite and martensite, Mater. Sci. Technol. 10 (1994) 209–214.
[40] S.M.C. van Bohemen, Bainite and martensite start temperature calculated with exponential carbon dependence, Mater. Sci. Technol. 28 (2012) 487–495.
[41] J.B. Seol, D. Raabe, P.P. Choi, Y.R. Im, C.G. Park, Atomic scale effects of alloying, partitioning, solute drag and austempering on the mechanical properties of high-carbon bainitic-austenitic TRIP steels, Acta Mater. 60 (2012) 6183–6199.
[42] B. Hutchinson, J. Hagström, O. Karlsson, D. Lindell, M. Tornberg, F. Lindberg, M. Thuvander, Microstructures and hardness of as-quenched martensites (0.1-0.5%C), Acta Mater. 59 (2011) 5845–5858.
[43] N. Ridley, H. Stuart, Lattice parameter anomalies at the curie point of pure iron, J. Phys. D. Appl. Phys. 1 (1968) 1291–1295.
[44] X.C. Xiong, B. Chen, M.X. Huang, J.F. Wang, L. Wang, The effect of morphology on the stability of retained austenite in a quenched and partitioned steel, Scr. Mater. 68 (2013) 321–324.
[45] Z.P. Xiong, A.A. Saleh, R.K.W. Marceau, A.S. Taylor, N.E. Stanford, A.G. Kostryzhev, E.V. Pereloma, Site-specific atomic-scale characterization of retained austenite in a

strip cast TRIP steel, Acta Mater. 134 (2017) 1–15.
[46] P.J. Jacques, J. Ladriere, F. Delannay, On the influence of interactions between phases on the mechanical stability of retained austenite in TRIP multiphase steels, Metall. Mater. Trans. A 32 (2001) 2759–2768.
[47] J. Hidalgo, K.O. Findley, M.J. Santofimia, Thermal and mechanical stability of retained austenite surrounded by martensite with different degrees of tempering, Mater. Sci. Eng. A 690 (2017) 337–347.
[48] J.G. Speer, E. De Moor, A.J. Clarke, Critical assessment 7: quenching and partitioning, Mater. Sci. Technol.-Lond. 31 (2015) 3–9.
[49] A.J. Clarke, J.G. Speer, M.K. Miller, R.E. Hackenberg, D.V. Edmonds, D.K. Matlock, F.C. Rizzo, K.D. Clarke, E. De Moor, Carbon partitioning to austenite from martensite of bainite during the quench and partition (Q&P) process: a critical assessment, Acta Mater. 56 (2008) 16–22.
[50] M.J. Santofimia, L. Zhao, R. Petrov, C. Kwakernaak, W.G. Sloof, J. Sietsma, Microstructural development during the quenching and partitioning process in a newly designed low-carbon steel, Acta Mater. 59 (2011) 6059–6068.
[51] Y. Toji, G. Miyamoto, D. Raabe, Carbon partitioning during quenching and partitioning heat treatment accompanied by carbide precipitation, Acta Mater. 86 (2015) 137–147.
[52] H.K.D.H. Bhadeshia, D.V. Edmonds, Bainite in silicon steels: new composition-property approach – Part 1, Met. Sci. 17 (1983) 411–419.